# Reconfigurable Holographic Surface: Holographic Beamforming for Metasurface-Aided Wireless Communications

Ruoqi Deng, *Student Member, IEEE*, Boya Di, *Member, IEEE*, Hongliang Zhang, *Member, IEEE*, Yunhua Tan, and Lingyang Song, *Fellow, IEEE*

***Abstract*—The future sixth generation (6G) wireless communications look forward to constructing a ubiquitous intelligent information network with high data rates. To fulfill such challenging visions, the reconfigurable holographic surface (RHS) is developed as a promising solution due to its capability of accurate multi-beam steering with low power consumption and hardware cost. Different from the conventional phase-controlled antennas, the RHS can control the radiation amplitude of the reference wave propagating on the metasurface by leveraging the holographic technique. The desired object waves can then be generated without complex phase-shifting circuits, enabling the convenient implementation of the transceiver. Such amplitude-controlled holographic beamforming triggers new challenges since a new beamforming scheme needs to be developed to handle the complex-domain optimization problem subject to the unconventional real-domain amplitude constraints, which makes the superposition of the radiation waves from different antenna elements difficult to tackle. In this letter, we consider an RHS-aided multi-user communication system with a base station equipped with an RHS. We formulate a sum rate maximization problem and design a novel amplitude-controlled algorithm to solve the problem. Simulation results verify the effectiveness of the proposed scheme.**

***Index Terms*—Reconfigurable holographic surface, holographic beamforming, multi-user communications.**

## I. Introduction

To enable a ubiquitous intelligent information network, the forthcoming sixth generation (6G) wireless communications put stringent requirements on antenna technologies such as capacity enhancement and low-power-consumption hardware components [1]. In the existing antenna technologies, the holographic antenna, a small-size and low-power-consumption planar antenna, has attracted increasing attention due to its capability of multi-beam steering with low manufacturing and hardware costs. Specifically, the holographic antenna utilizes meta patches to construct the *holographic pattern* on the surface, which records the interference between the reference wave and the desired object wave based on the interference principle. The radiation characteristics of the reference wave can then be changed by the holographic pattern to generate the desired radiation pattern.

However, the exponentially increasing mobile devices pose great challenges to the conventional holographic antenna since its radiation pattern is fixed once the holographic pattern is constructed. Fortunately, the emerging reconfigurable holographic surface (RHS) shows great potential to make up for the deficiency in the conventional holographic antenna due to the controllability of the metamaterial [2]. The RHS is an ultra-thin and lightweight surface antenna inlaid with numerous metamaterial radiation elements. Specifically, the reference wave generated by the feed excites the metasurface in the form of a surface wave,[1] enabling the compact design of the RHS based on the printed-circuit-board (PCB) technology. According to the holographic pattern, each element can control the *radiation amplitude* of the reference wave electrically to generate the desired radiation pattern[2]. Therefore, the RHS can achieve dynamic beamforming without heavy mechanical moving apparatus and complex phase-shifting circuits. It can be installed on mobile platforms (such as trains, aircrafts, and vehicles) to provide high-throughput data services[3].

In the literature, existing works on the RHS can be roughly divided into hardware component design [2] and radiation pattern control [3]. In [2], a PCB-based parallel-plate waveguide RHS capable of generating multi-beam radiation patterns has been presented. In [3], the radiation pattern control algorithms of the RHS have been developed for sidelobe suppression. However, most works only demonstrate the viability of the RHS to achieve dynamic multi-beam steering. None of them have studied the influence of holographic beamforming on system performance.

This letter is the first to consider multi-user communications aided by the RHS. We propose a hybrid beamforming scheme to support the communications between a BS equipped with an RHS and multiple mobile users. Specifically, the digital beamforming at the BS and the holographic beamforming at the RHS are jointly optimized to maximize the sum rate. This is a non-trivial task due to the following two reasons. *First*, the traditional phase-controlled analog beamforming scheme is not applicable to the amplitude-controlled holographic beamforming. A new beamforming scheme needs to be developed to handle the complex-domain optimization problem subject to the unconventional real-domain amplitude constraints, coupled with the superposition of the radiation waves from different radiation elements. *Second*, the coupling between all the radiation elements simultaneously with the propagating surface wave complicates the holographic beamforming design. To tackle these challenges, we design a novel amplitude-controlled algorithm where the closed-form optimal holographic beamforming scheme is also derived.

## II. Reconfigurable Holographic Surface

In this section, we introduce the physical structure and the holographic principle of the RHS.

### A. Physical Structure

The RHS is a kind of special leaky-wave antenna. It mainly consists of four parts, i.e., $K$ feeds, a parallel-plate waveguide, a planar array of $M \times N$ discrete, sub-wavelength metamaterial radiation elements, and radiation amplitude controllers as shown in Fig. 1(a). Specifically, the feeds are embedded in the bottom layer of the RHS to generate the reference waves carrying intended signals for receivers. The generated

Manuscript received December 11, 2020; revised March 1, 2021; accepted April 27, 2021. Date of publication May 14, 2021; date of current version July 8, 2021. This work was supported in part by the National Natural Science Foundation of China under Grants 61931019, 61625101, 61829101, 61941101, and 61911540076. The review of this article was coordinated by Dr. P. Lin. *(Corresponding author: Lingyang Song.)*

Ruoqi Deng, Boya Di, Yunhua Tan, and Lingyang Song are with the Department of Electronics, Peking University, Beijing 100871, China (e-mail: ruoqi.deng@pku.edu.cn; diboya92@gmail.com; tanggeric@pku.edu.cn; lingyang.song@pku.edu.cn).

Hongliang Zhang is with the Department of Electrical Engineering, Princeton University, Princeton, NJ 08544 USA (e-mail: hongliang.zhang92@gmail.com).

Digital Object Identifier 10.1109/TVT.2021.3079465

[1]The surface wave refers to the electromagnetic wave bound to the surface of a guiding wave structure, and propagates along the guiding wave structure.

[2]The amplitude-controlled beamforming is commonly used in the RHS [3].

[3]The RHS can also be utilized in hybrid satellite-terrestrial networks for global connectivity and high-capacity communications with satellites [4].

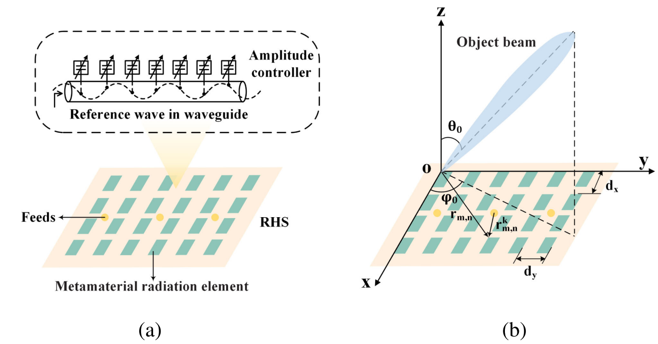


Fig. 1. Illustration of the RHS. (a) Schematic structure of RHS. (b) Geometrical relation between the RHS and object beam.

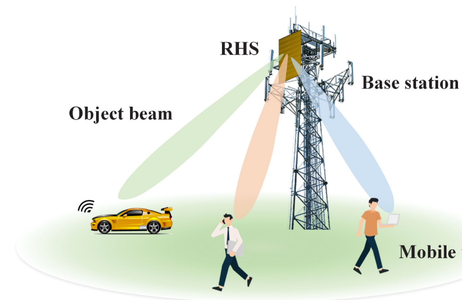


Fig. 2. Reconfigurable holographic surface-aided communication system.

reference waves are injected into the waveguide directly. Such a structure enables an ultra-thin RHS compared to traditional antenna arrays where the feeds are usually bulky and outside the antenna surface. The parallel-plate waveguide plays a role of a guiding wave structure and is the propagation medium of the reference wave. It bounds and guides the reference wave to propagate on its surface in the form of a surface wave. The metamaterial radiation element is made of artificial composite material with supernormal electromagnetic properties or structures, whose electromagnetic response (such as radiation amplitude) can be intelligently controlled by the magnetic or electric bias field [5]. In the RHS, there are numerous metamaterial radiation elements on the surface of the waveguide. Each radiation element is excited by the reference waves propagating on the waveguide beneath the elements and controlled by the radiation amplitude controller.

## B. Holographic Principle

The main characteristic of the RHS is to construct the *holographic pattern*, which records the interference between the reference wave and the object wave according to the holographic interference principle. Utilizing the holographic pattern, the RHS can effectively control the leakage of the reference wave to obtain the object wave.

We adopt the Cartesian coordinate where the $xoy$ plane coincides with the RHS, and the $z$-axis is vertical to the RHS as shown in Fig. 1(b). At the $(m, n)$-th radiation element, the desired wave propagates in the direction $(\theta_0, \varphi_0)$ is $\Psi_{obj}(\mathbf{r}_{m,n}, \theta_0, \varphi_0) = \exp(-j\mathbf{k}_f(\theta_0, \varphi_0) \cdot \mathbf{r}_{m,n})$, and the reference wave generated by feed $k$ is $\Psi_{ref}(\mathbf{r}^k_{m,n}) = \exp(-j\mathbf{k}_s \cdot \mathbf{r}^k_{m,n})$, where $\mathbf{k}_f(\theta_0, \varphi_0)$ is the desired directional propagation vector in free space, $\mathbf{k}_s$ is the propagation vector of the reference wave, $\mathbf{r}_{m,n}$ is the position vector of the $(m, n)$-th radiation element, and $\mathbf{r}^k_{m,n}$ the distance vector from the feed $k$ to the $(m, n)$-th radiation element. The interference between the reference wave and the desired object wave is defined as

$$\Psi_{intf}(\mathbf{r}^k_{m,n}, \theta_0, \varphi_0) = \Psi_{obj}(\mathbf{r}_{m,n}, \theta_0, \varphi_0)\Psi^*_{ref}(\mathbf{r}^k_{m,n}). \tag{1}$$

Therefore, when the holographic pattern is excited by the reference wave, we have $\Psi_{intf}\Psi_{ref} \propto \Psi_{obj}|\Psi_{ref}|^2$, such that the wave propagating in the direction $(\theta_0, \varphi_0)$ is generated.

To record the interference pattern, the RHS adopts an amplitude controlling method to construct the holographic pattern instead of conventional phase shifting. Note that the real part of $\Psi_{intf}(\mathbf{r}^k_{m,n}, \theta_0, \varphi_0)$, i.e., $\cos(\mathbf{k}_f(\theta_0, \varphi_0) \cdot \mathbf{r}_{m,n} - \mathbf{k}_s \cdot \mathbf{r}^k_{m,n})$, contains the full information of both the object wave and the reference wave. The normalized radiation amplitude of the $(m, n)$-th radiation element to generate the object wave with the radiation direction of $(\theta_0, \varphi_0)$ can be given by

$$\mathrm{M}(\mathbf{r}^k_{m,n}, \theta_0, \varphi_0) = \frac{\mathrm{Re}[\Psi_{intf}(\mathbf{r}^k_{m,n}, \theta_0, \varphi_0)] + 1}{2}. \tag{2}$$

According to (2), when the phase shift of the reference wave in a radiation element is significantly different from that of the object wave, it is required that the element should radiate little energy into free space. On the contrary, if the reference wave's phase shift is close to the object wave's phase shift, the element is required to radiate much energy into free space to generate desired radiation patterns. Therefore, unlike the traditional phase-controlled beamforming relying on controlling the phase of the electromagnetic wave propagating along each antenna of the array, the holographic beamforming is realized by controlling the radiation amplitude of each element without complex phase-shifting circuits.

# III. System Model

In this section, we first introduce the RHS-aided multi-user communication system and propose a hybrid beamforming scheme. The communication model is then presented.

## A. Scenario Description

Consider a downlink multi-user communication system as shown in Fig. 2, where a BS transmits data streams to $L$ mobile users denoted by $\mathcal{L} = \{1, \ldots, l, \ldots, L\}$. Each mobile user requires a single data stream from the BS. Without loss of generality, it is assumed that each mobile user is equipped with $J$ antennas and a single RF receive chain. Due to the mobility of users, high requirements are put forward to the transmit antenna array's capability of multi-beam steering. Therefore, we consider equipping an RHS on the BS by leveraging the holographic technique to achieve accurate beamforming without using bulky mechanics and phase-shifting circuits[4].

## B. Hybrid Beamforming Scheme

Since the RHS does not have any digital processing capability, the BS needs to process the signal at the baseband. Without loss of generality, we assume that the BS first encodes $L$ different data streams via a digital beamformer $\mathbf{V} \in \cdot^{K\times L}$, and then up-converts the processed signals to the carrier frequency by passing through RF chains. Each RF chain is connected with a feed of the RHS, i.e., the number of RF chains is the same as the number of feeds $K$[5]. Each RF chain sends the

[4]The RHS first performs beam training [6] to track the users and then transmits signals to users through holographic beamforming.

[5]It is required that the number of RF chains in the hybrid architecture should be greater than or equal to the number of active data streams [7]. In other words,

up-converted signals to its connected feed. The feed then transforms the high frequency current into electromagnetic wave (which is also called reference wave) propagating on the RHS. The radiation amplitude of the reference wave at each radiation element is controlled via a holographic beamformer $\{\mathrm{M_{m,n}}\}$ to generate desired directional beams.

### C. Communication Model

Denote the intended signal vector for $L$ mobile users as $\mathbf{s} \in \cdot^{L\times 1}$, and thus, the transmitted signals of the BS is $\mathbf{Vs}$. The final signals received by mobile user $l$ can be given by

$$y_l = \mathbf{W}_l^H \mathbf{H}_l \mathbf{M} \mathbf{V}_l s_l + \mathbf{W}_l^H \mathbf{H}_l \mathbf{M} \sum_{l' \neq l} \mathbf{V}_{l'} s_{l'} + \mathbf{W}_l^H \mathbf{z}_l, \quad (3)$$

where $\mathbf{H}_l \in \cdot^{J\times MN}$ is the matrix of complex channel gains from the RHS to the $l$-th user's antennas, $\mathbf{M}$ is an $MN \times K$ matrix composed of element $\{\mathrm{M}_{m,n} \cdot e^{-j\mathbf{k}_s \cdot \mathbf{r}_{m,n}^k}\}$, $e^{-j\mathbf{k}_s \cdot \mathbf{r}_{m,n}^k}$ is the phase of the reference wave, $\mathbf{V}_l$ is the $l$-th column of $\mathbf{V}$, and $\mathbf{z}_l \sim \mathcal{CN}(\mathbf{0}, \sigma^2 \mathbf{I}_J)$ is the additive white Gaussian noise. $\mathbf{W}_l$ is a $J \times 1$ RF combiner at each mobile user, implemented using phase shifters such that $|\mathbf{W}_l(j)|^2 = 1$. For convenience, we consider the uniform linear phased array at each mobile user, where $\mathbf{W}_l = [1, e^{jk_f d_s \sin\phi_l}, \ldots, e^{jk_f (J-1) d_s \sin\phi_l}]^T$, $d_s$ is the distance between antennas of the mobile user, and $\phi_l$ is the angle of arrival of the signals with respect to the antenna array at mobile user $l$. Therefore, the achievable rate of mobile user $l$ can be given by

$$R_l = \log_2 \left( 1 + \frac{|\mathbf{W}_l^H \mathbf{H}_l \mathbf{M} \mathbf{V}_l|^2}{J\sigma^2 + \sum_{l' \neq l} |\mathbf{W}_l^H \mathbf{H}_l \mathbf{M} \mathbf{V}_{l'}|^2} \right). \quad (4)$$

## IV. Problem Formulation and Algorithm Design

In this section, we first formulate a sum rate maximization problem in the RHS-aided multi-user communication system. We then develop a joint optimization algorithm to solve it.

### A. Sum Rate Maximization Problem Formulation

We aim to maximize the achievable rates of all mobile users by optimizing the digital beamformer $\mathbf{V}$ and the holographic beamformer $\{\mathrm{M}_{m,n}\}$, as formulated below:

$$\max_{\{\mathbf{V}, \mathrm{M}_{m,n}\}} \sum_{l=1}^{L} R_l \quad \text{s.t. } \mathrm{Tr}(\mathbf{V}^H \mathbf{V}) \leq P_T,\ 0 \leq \mathrm{M}_{m,n} \leq 1, \quad (5)$$

where $P_T$ is the total transmit power of the BS.

Problem (5) is different from traditional phase-controlled beamforming design in multi-user MIMO systems since it is a complex-domain optimization problem subject to unconventional real-domain amplitude constraints, coupled with the superposition of the radiation waves from different radiation elements. Existing algorithms do not work well since the traditional analog beamformer is a complex-valued matrix with complex-domain phase constraints [8]. To tackle the above challenges, we consider utilizing the affine characteristic of linear functions to eliminate the non-convex terms in (4). Specifically, the modulus of the inner product of a real-valued matrix with other matrices (e.g., the term $|\mathbf{W}_l^H \mathbf{H}_l \mathbf{M} \mathbf{V}_l|$ given in (4)) can be well approximated by a linear function of its elements. The holographic beamforming optimization problem can then be reformulated as a series of convex optimization subproblems with closed-form optimal solutions.

the number of feeds should also be no less than the number of active data streams, i.e., $K \geq L$.

To solve problem (5) efficiently, we decompose it into two subproblems, i.e., digital beamforming to optimize $\mathbf{V}$ and holographic beamforming to optimize $\{\mathrm{M}_{m,n}\}$. In the next subsections, we first present two algorithms to solve these two subproblems, respectively. The overall iterative optimization algorithm is then summarized.

### B. Digital Beamforming Design

Since the ZF digital beamformer can obtain a near-optimal solution, we consider ZF beamforming together with power allocation as the low-dimensional digital beamformer at the BS to alleviate the inter-user interference [8]. The digital beamformer at the BS can then be given by

$$\mathbf{V} = \mathbf{Q}^H (\mathbf{Q}\mathbf{Q}^H)^{-1} \mathbf{P}^{\frac{1}{2}} = \widetilde{\mathbf{V}} \mathbf{P}^{\frac{1}{2}}, \quad (6)$$

where $\mathbf{Q} = (\mathbf{M}^H \mathbf{H}_1^H \mathbf{W}_1, \ldots, \mathbf{M}^H \mathbf{H}_L^H \mathbf{W}_L)^H \in \mathbb{C}^{L\times K}$, $\mathbf{P} = \mathrm{diag}(p_1, \ldots, p_L)$ is a diagonal matrix, and $p_l$ is the received power at mobile user $l$. Utilizing the properties of ZF beamforming, i.e., $\mathbf{W}_l^H \mathbf{H}_l \mathbf{M} \mathbf{V}_l = \sqrt{p_l}$ and $\mathbf{W}_l^H \mathbf{H}_l \mathbf{M} \mathbf{V}_{l'} = 0, \forall l' \neq l$, the digital beamforming subproblem can be simplified as a power allocation problem given as below:

$$\max_{\{p_l\}} \sum_{l=1}^{L} \log_2 \left( 1 + \frac{p_l}{J\sigma^2} \right) \text{ s.t. } \mathrm{Tr}(\mathbf{P}^{\frac{1}{2}} \widetilde{\mathbf{V}}^H \widetilde{\mathbf{V}} \mathbf{P}^{\frac{1}{2}}) \leq P_T. \quad (7)$$

The optimal $\{p_l^*\}$ can be obtained by water-filling as $p_l^* = \frac{1}{\mu_l} \max\{\frac{1}{\nu} - J\mu_l\sigma^2, 0\}$, where $\mu_l$ is the $l$-th diagonal element of $\widetilde{\mathbf{V}}^H \widetilde{\mathbf{V}}$, and $\nu$ is a normalized factor satisfying $\sum_{l=1}^{L} \max\{\frac{1}{\nu} - J\mu_l\sigma^2, 0\} = P_T$. The digital beamformer $\mathbf{V}$ can then be derived from the optimal $\{p_l^*\}$ based on (6).

### C. Holographic Beamforming Design

To solve the non-convex subproblem of holographic beamforming, we convert it into a sequence of convex subproblems to derive the optimal holographic beamforming scheme.

*1) Problem Reformulation:* The key idea is to eliminate the non-convex ratio (i.e., $\frac{|\mathbf{W}_l^H \mathbf{H}_l \mathbf{M} \mathbf{V}_l|^2}{J\sigma^2 + \sum_{l' \neq l} |\mathbf{W}_l^H \mathbf{H}_l \mathbf{M} \mathbf{V}_{l'}|^2}$) in $R_l$ and recast $R_l$ into the maxima of a concave function based on the fractional programming technique. This equivalent form allows an iterative convex optimization algorithm to optimize the holographic beamforming scheme.

We first write the subproblem as

$$\max_{\{\mathrm{M}_{m,n}\}} \sum_{l=1}^{L} \log_2 \left( 1 + \frac{|\sum_{m,n} \mathrm{M}_{m,n} b_{m,n}^{l,l}|^2}{J\sigma^2 + \sum_{l' \neq l} |\sum_{m,n} \mathrm{M}_{m,n} b_{m,n}^{l,l'}|^2} \right) \quad (8a)$$

$$\text{s.t.} \quad 0 \leq \mathrm{M}_{m,n} \leq 1, \forall m, n, \quad (8b)$$

where $b_{m,n}^{l,l'} = \sum_{j,k} \overline{\mathbf{W}_l(j)} \cdot h_{m,n}^{l,j} e^{-j\mathbf{k}_s \cdot \mathbf{r}_{m,n}^k} v_{k,l'}$, and $\overline{\mathbf{W}_l(j)}$ is the conjugate of $\mathbf{W}_l(j)$. $h_{m,n}^{l,j}$ is denotes the channel between the $(m,n)$-th radiation element of the RHS and the $j$-th antenna of mobile user $l$, and $v_{k,l'}$ is the $l'$-th element in row $k$ of matrix $\mathbf{V}$.

*Lemma 1.* Define $\mathbf{b}_l \in \cdot^{MN\times 1}$ as the vectorization of $b_{m,n}^{l,l}$ with respect to subscripts $m, n$, the linear approximation of the term $|\sum_{m,n} \mathrm{M}_{m,n} b_{m,n}^{l,l}|$ can be given by $\sum_{m,n} \mathrm{M}_{m,n} c_{m,n}^l$, where $c_{m,n}^l = \sqrt{\eta_l} u_{m,n}^l$, $\eta_l$ is the largest eigenvalue of matrix $\mathrm{Re}(\mathbf{b}_l)[\mathrm{Re}(\mathbf{b}_l)]^T + \mathrm{Im}(\mathbf{b}_l)[\mathrm{Im}(\mathbf{b}_l)]^T$, and $u_{m,n}^l$ is the $[(m-1)N+n]$-th element of the eigenvalue corresponding to $\eta_l$.

*Proof:* See Appendix A.

*Lemma 2.* The achievable rate of each user $R_l(\mathrm{M}_{m,n})$ shown in (4) is equivalent to $\max_{\{\gamma_l, \delta_l\}} A_l(\mathrm{M}_{m,n}, \boldsymbol{\gamma}, \boldsymbol{\delta})$ [9], where $\gamma_l$ and $\delta_l$ are the auxiliary variables corresponding to each $l$, and

**Algorithm 1:** Holographic Beamforming Design.

**Input**: The position of each mobile user with respect to the origin $\{(\theta_l, \varphi_l)\}$, the digital beamformer $\mathbf{V}$.
Initialize $\{\mathrm{M}_{m,n}\}$;
**repeat**
  *Step 1*: Compute $\boldsymbol{\gamma}^*$ and $\boldsymbol{\delta}^*$ by (10) and (11);
  *Step 2*: Compute $\{\mathrm{M}_{m,n}\}$ by (12) ;
  *Step 3*: Update $\boldsymbol{\lambda}$ by the subgradient method;
**until** *Convergence*;
**Output**: The optimal holographic beamformer $\{\mathrm{M}^*_{m,n}\}$.

$A_l(\mathrm{M}_{m,n}, \boldsymbol{\gamma}, \boldsymbol{\delta}) = \frac{1}{\log 2}[\log(1+\gamma_l) - \gamma_l + 2\delta_l \sum_{m,n} \mathrm{M}_{m,n} c^l_{m,n} \cdot \sqrt{1+\gamma_l} - \delta_l^2 (J\sigma^2 + \sum_{l'=1}^{L} |\sum_{m,n} \mathrm{M}_{m,n} b^{l,l'}_{m,n}|^2)]$.

Therefore, problem (8) can be reformulated as

$$\max_{\{\mathrm{M}_{m,n}, \gamma_l, \delta_l\}} \sum_{l=1}^{L} A_l \quad \text{s.t.} \quad 0 \le \mathrm{M}_{m,n} \le 1, \forall m, n. \tag{9}$$

*2) Holographic Beamforming Design:* To obtain the optimal solution of problem (9), we iteratively optimize the variables $\boldsymbol{\gamma}$, $\boldsymbol{\delta}$, and $\{\mathrm{M}_{m,n}\}$. The derivation of optimal solutions with respect to these variables is illustrated as below.

Given the variables $\{\mathrm{M}_{m,n}\}$, by setting $\partial A_l / \partial \gamma_l$ to 0, we can obtain the optimal $\boldsymbol{\gamma}^*$, which can be expressed as

$$\gamma_l^* = \frac{(\sum_{m,n} \mathrm{M}_{m,n} c^l_{m,n})^2}{J\sigma^2 + \sum_{l' \neq l} |\sum_{m,n} \mathrm{M}_{m,n} b^{l,l'}_{m,n}|^2}, \tag{10}$$

and the optimal $\boldsymbol{\delta}^*$ can be obtained by setting $\partial A_l / \partial \delta_l$ to 0, which can be expressed as

$$\delta_l^* = \frac{(\sum_{m,n} \mathrm{M}_{m,n} c^l_{m,n}) \sqrt{1+\gamma_l}}{J\sigma^2 + \sum_{l'=1}^{L} |\sum_{m,n} \mathrm{M}_{m,n} b^{l,l'}_{m,n}|^2}. \tag{11}$$

Given the auxiliary variables $\boldsymbol{\gamma}$ and $\boldsymbol{\delta}$, the optimal $\mathrm{M}^*_{m,n}$ can be obtained by solving the convex problem (9). Specifically, we utilize the Lagrangian dual from relaxing the constraints $\{0 \le \mathrm{M}_{m,n} \le 1, \forall m, n\}$ with multipliers. Denote $\boldsymbol{\lambda}$ as the Lagrangian multipliers associated the constraints. The Lagrangian associated with holographic beamforming design is $\boldsymbol{\mathcal{L}}(\mathrm{M}_{m,n}, \boldsymbol{\lambda}) = \sum_{l=1}^{L} A_l - \sum_{m,n} \lambda_{m,n} (\mathrm{M}^2_{m,n} - \mathrm{M}_{m,n})$. By setting $\partial \boldsymbol{\mathcal{L}} / \partial \mathrm{M}_{m,n}$ to 0, the optimal closed-form holographic beamforming scheme $\{\mathrm{M}^*_{m,n}\}$ can be obtained by solving the system of linear equations given in (12).

$$\sum_{m,n} \left[ \sum_{l=1}^{L} \delta_l^2 \sum_{l'=1}^{L} (b^{l,l'}_{m_1,n_1} \overline{b^{l,l'}_{m,n}} + b^{l,l'}_{m,n} \overline{b^{l,l'}_{m_1,n_1}}) \right] \mathrm{M}_{m,n}$$
$$= \sum_{l=1}^{L} 2\delta_l \sqrt{1+\gamma_l} c^l_{m_1,n_1} + \log 2 \cdot \lambda_{m_1,n_1} (1 - 2\mathrm{M}_{m_1,n_1}), \forall m_1, n_1. \tag{12}$$

The above optimization process is composed of multiple iterations in each of which $\boldsymbol{\gamma}$, $\boldsymbol{\delta}$ and $\{\mathrm{M}_{m,n}\}$ are updated accordingly. The whole iterative holographic beamforming design optimization algorithm is summarized in Algorithm 1.

## D. Overall Algorithm Description

Based on the algorithms presented in the previous two subsections, we design a joint sum rate optimization algorithm to solve problem (5) in an iterative manner. Specifically, the digital beamformer $\mathbf{V}$ can be obtained by (6) while keeping the holographic beamformer fixed. The holographic beamformer $\{\mathrm{M}_{m,n}\}$ is then optimized by Algorithm 1. The optimized digital beamformer and holographic beamformer are set as the initial solution. In each subsequent iteration, the two subproblems are solved alternatively. The iterations are completed until the value difference of the sum rate between two adjacent iterations is less than a predefined threshold. The proof of convergence for Algorithm 1 and the overall algorithm is similar to our previous work [10] and omitted here due to the space limitation.

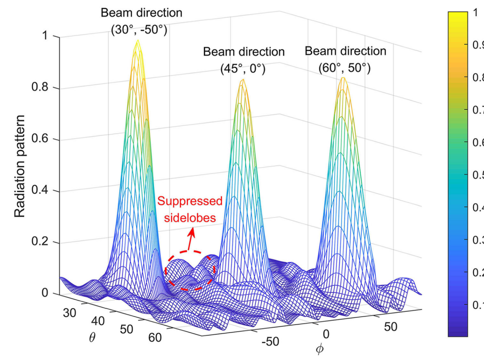


Fig. 3. The radiation pattern of the RHS.

## V. Simulation Results

In this section, we evaluate the performance of the proposed joint sum rate optimization algorithm for the RHS-aided multi-user system. Simulation parameters are set as below. The carrier frequency $f$ is 10 GHz[6], and the value of the reference wave's propagation vector $|\mathbf{k}_s|$ is $\sqrt{3}|\mathbf{k}_f|$, i.e., $2\sqrt{3}\pi f/c$, where $c$ is the speed of light. The element spacing of the RHS $d_x$ and $d_y$ are both set as 0.75 cm. The height of the BS is 50 m, and the transmit power $P_T$ is 1 W [10]. The propagation environment between the BS and each user is modeled as a sparse millimeter wave channel with $I$ paths, i.e., $\mathbf{H}_l = \sqrt{\frac{MNJ}{I}} \sum_{i=1}^{I} \alpha^i_l \mathbf{a}_r(\phi^l_{r_i}) \mathbf{a}_t(\theta^l_{t_i}, \varphi^l_{t_i})^H$, where $\alpha^i_l$ is the complex gain of the $i$-th path, $\phi^l_{r_i}$ and $(\theta^l_{t_i}, \varphi^l_{t_i})$ are the physical angle of arrival and angle of departure, respectively. $\mathbf{a}_r(\phi^l_{r_i})$ and $\mathbf{a}_t(\theta^l_{t_i}, \varphi^l_{t_i})$ are the antenna array response vectors of the user $l$ and the BS, respectively [7]. For simplicity, we consider one line-of-sight path and one none-line-of-sight path between the BS and each user [6].

Fig. 3 shows the normalized radiation pattern of the RHS based on the proposed hybrid beamforming scheme. The desired radiation directions $\{(\theta_i, \phi_i)\}$ are set as $\{(30^\circ, -50^\circ), (45^\circ, 0^\circ), (60^\circ, 50^\circ)\}$. We observe that directions of the beams generated by the RHS are the same as the desired beam directions with low sidelobe levels (i.e., about $-9$ dB). This demonstrates that through controlling the radiation amplitude of each radiation element, the RHS has the capability of accurate multi-beam steering.

Fig. 4 illustrates the sum rate versus the size of the RHS, i.e., $M$[7] It can be seen that the sum rate increases rapidly with a small value of $M$ and gradually flattens as $M$ continues to grow. The main reason is that the increment of $M$ first contributes to space multiplexing gain, and then only contributes to power gain due to the high correlation between different channel links.

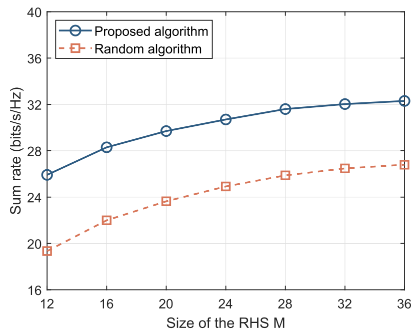


Fig. 4. The sum rate versus the size of the RHS.

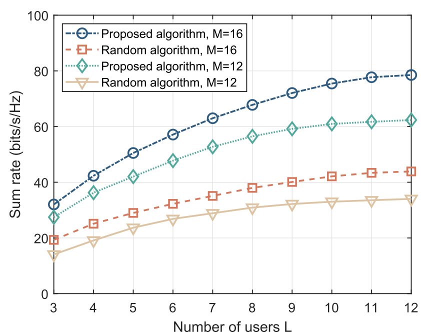


Fig. 5. The sum rate versus the number of users.

Fig. 5 depicts the sum rate versus the number of users,[8] i.e., $L$. We observe that the sum rate first increases and then gradually saturates as $L$ grows. This is because the spatial degrees of freedom of the channels increase with $L$. However, since the increasing $L$ results in the decrease of the transmit power to each user, the multi-user gain is offset by the decreasing SINR of each user when $L$ continues to grow. Moreover, both Fig. 4 and Fig. 5 show that the proposed joint sum rate optimization algorithm outperforms the benchmark, i.e., the random algorithm where the ZF digital beamforming is first performed, followed by a random algorithm to solve the holographic beamforming subproblem.

## VI. Conclusion

In this letter, we have developed an RHS-aided multi-user communication scheme where a BS equipped with an RHS communicates with users. To maximize the sum rate, we have proposed an iterative algorithm jointly optimizing the digital beamforming at the BS and the holographic beamforming at the RHS. The closed-form optimal holographic beamforming scheme has also been derived. Simulation results reveal that the RHS has the capability of accurate multi-beam steering with low sidelobe levels (i.e., about -9 dB) through amplitude controlling. Besides, a moderate sized RHS is enough to achieve a satisfactory sum rate.

[6]The commercial prototypes of the RHS operating over high frequency bands have been developed by Kymeta [4].

[7]We set $M = N$ and adopt $M$ to represent the size of the RHS.

[8]Without loss of generality, it is assumed that the mobile users are randomly deployed within a circle of radius 50 m centering at the BS.

## Appendix A

Define $\tilde{\mathbf{M}}$ as the vectorization of the holographic pattern $\{\mathrm{M}_{m,n}\}$, $|\sum_{m,n}\mathrm{M}_{m,n}b_{m,n}^{l,l}|$ can then be reformulated as $\sqrt{\tilde{\mathbf{M}}^H\{\mathrm{Re}(\mathbf{b}_l)[\mathrm{Re}(\mathbf{b}_l)]^T+\mathrm{Im}(\mathbf{b}_l)[\mathrm{Im}(\mathbf{b}_l)]^T\}\tilde{\mathbf{M}}}$. Since the matrix $\mathrm{Re}(\mathbf{b}_l)[\mathrm{Re}(\mathbf{b}_l)]^T+\mathrm{Im}(\mathbf{b}_l)[\mathrm{Im}(\mathbf{b}_l)]^T$ is a symmetric matrix with rank 2, its spectral decomposition can be given by $\eta_l\mathbf{u}_{l,1}\mathbf{u}_{l,1}^H+\xi_l\mathbf{u}_{l,2}\mathbf{u}_{l,2}^H\approx\eta_l\mathbf{u}_{l,1}\mathbf{u}_{l,1}^H$, where $\eta_l\geq\xi_l$ are the two nonzero eigenvalues, $\mathbf{u}_{l,1}$, $\mathbf{u}_{l,2}$ are the corresponding eigenvectors. $|\sum_{m,n}\mathrm{M}_{m,n}b_{m,n}^{l,l}|$ can then be approximated by $\sqrt{\tilde{\mathbf{M}}^H(\eta_l\mathbf{u}_{l,1}\mathbf{u}_{l,1}^H)\tilde{\mathbf{M}}}=\sqrt{\eta_l}\tilde{\mathbf{M}}^H\mathbf{u}_{l,1}=\sum_{m,n}\mathrm{M}_{m,n}c_{m,n}^l$.

## References

[1] S. Zhang *et al.*, “Envisioning device-to-device communications in 6G,” *IEEE Netw.*, vol. 34, no. 3, pp. 86–91, Mar. 2020.

[2] O. Yurduseven *et al.*, “Dual-polarization printed holographic multibeam metasurface antenna,” *IEEE Antennas Wireless Propag. Lett.*, vol. 16, pp. 2738–2741, Aug. 2017.

[3] M. C. Johnson *et al.*, “Sidelobe canceling on a reconfigurable holographic metamaterial antenna,” in *Proc. Int. Conf. Electromagn. Adv. Appl.*, Palm Beach, FL, USA, 2014, pp. 806–809.

[4] Kymeta “Metamaterial-surface flat-panel antenna technology,” Jun. 2019. [Online]. Avilable: https://www.kymetacorp.com/wp-content/uploads/2019/06/Metamaterial-Surface-Antenna-Technology.pdf

[5] H. Hashida *et al.*, “Intelligent reflecting surface placement optimization in air-ground communication networks toward 6G,” *IEEE Wireless Commun.*, vol. 27, no. 6, pp. 146–151, Dec. 2020.

[6] D. Zhang *et al.*, “Fast beam tracking for millimeter-wave systems under high mobility,” in *Proc. IEEE Int. Conf. Commun.*, Shanghai, China, 2019, pp. 1–6.

[7] F. Sohrabi *et al.*, “Hybrid digital and analog beamforming design for large-scale MIMO systems,” in *Proc. IEEE Int. Conf. Acoustics, Speech Signal Process.*, Brisbane, QLD, 2015, pp. 2929–2933.

[8] B. Di *et al.*, “Hybrid beamforming for reconfigurable intelligent surface based multi-user communications: Achievable rates with limited discrete phase shifts,” *IEEE J. Sel. Areas Commun.*, vol. 38, no. 8, pp. 1809–1822, Aug. 2020.

[9] K. Shen *et al.*, “Load and interference aware joint cell association and user scheduling in uplink cellular networks,” in *Proc. IEEE Int. Workshop Signal Process. Adv. Wireless Commun.*, Edinburgh, U.K., 2016, pp. 1–5.

[10] R. Deng *et al.*, “Ultra-dense LEO satellite offloading for terrestrial networks: How much to pay the satellite operator?,” *IEEE Trans. Wireless Commun.*, vol. 19, no. 10, pp. 6240–6254, Oct. 2020.